Potential of bismuth nanoparticles embedded in a glass matrix for spectral-selective thermo-optical devices

M. Jiménez de Castro, F. Cabello, J. Toudert, R. Serna, and E. Haro-Poniatowski

Citation: Applied Physics Letters **105**, 113102 (2014); doi: 10.1063/1.4895808

View online: http://dx.doi.org/10.1063/1.4895808

View Table of Contents: http://scitation.aip.org/content/aip/journal/apl/105/11?ver=pdfcov

Published by the AIP Publishing

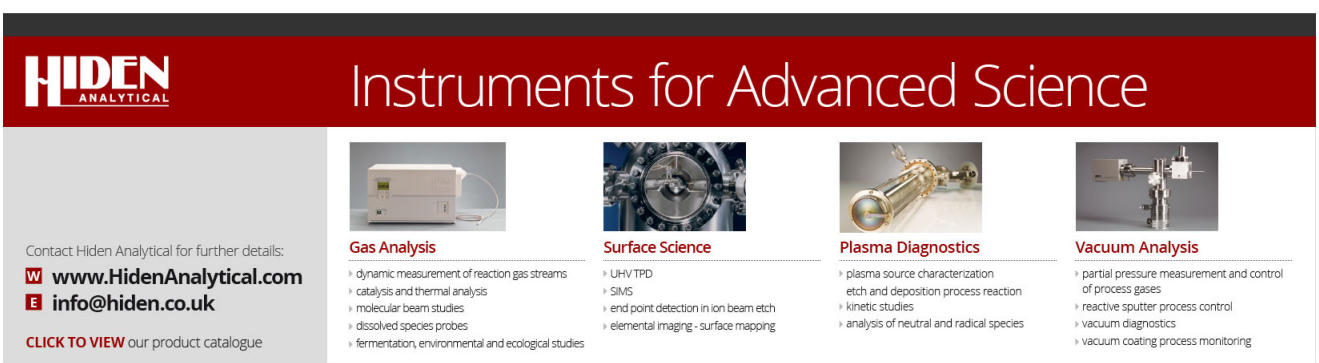

Potential of bismuth nanoparticles embedded in a glass matrix for spectral-selective thermo-optical devices

M. Jiménez de Castro,[1,a)] F. Cabello,[1] J. Toudert,[1,b)] R. Serna,[1] and E. Haro-Poniatowski[2]
[1]*Laser Processing Group, Instituto de Óptica, CSIC, Serrano 121, 28006 Madrid, Spain*
[2]*Departamento de Física, Universidad Autónoma Metropolitana Iztapalapa, Apartado Postal 55-534, México 09340, DF, Mexico*

(Received 16 May 2014; accepted 30 August 2014; published online 15 September 2014)

The optical transmission at a fixed visible wavelength of Bi nanoparticles embedded in a dielectric is known to show a sharp hysteretic evolution as a function of the temperature due to the reversible melting-solidification of the nanoparticles. In this work, we explore the temperature-dependent optical response of Bi nanoparticles embedded in a doped germanate glass (GeO_2-Al_2O_3-Na_2O) in a broad range from the visible to the near infrared. The transmission contrast induced by melting of the nanoparticles is shown to be strongly wavelength-dependent and evolves from positive to negative as the wavelength increases. This behaviour is well modelled using effective medium calculations, assuming that the nanoparticles size, shape, and distribution are unmodified upon melting, while their dielectric function turns from that of solid Bi to that of liquid Bi thus modifying markedly their optical response. These results open a route to the spectral tailoring of the thermo-optical response of Bi nanoparticles-based materials, which can be profitable for the engineering of wavelength-selective thermo-optical modulators and filters with optimized amplitude of modulation and wavelength dependence. © *2014 AIP Publishing LLC*.
[http://dx.doi.org/10.1063/1.4895808]

During the last years, much interest has been devoted to the development of active nanomaterials whose optical response could be tuned reversibly in the desired spectral range by means of an external optical,[1] electrical,[2–4] or thermal[5,6] excitation. Direct applications aimed for such materials are optical modulators and filters with strong amplitude of modulation or strong sensitivity to external excitation. Nanomaterials based on plasmonic nanostructures have the possibility to fulfil these two requirements. Indeed, the spectral response of plasmonic nanostructures can readily be tailored by fabricating them with the adequate shape, size, and surrounding medium. Besides, a relevant modulation of the plasmonic response of the nanostructures is also achievable, provided the material they are made of is sensitive to an external excitation. Such active behaviour cannot be achieved using Ag or Au, thus requiring the development of nanostructures based on some of the so-called "alternative plasmonic materials."[7,8] Among the long list of such materials, poor metals such as Ga,[9,10] Sn,[11] or Bi[12] have the capability of displaying plasmonic or plasmonic-like effects in the near ultraviolet-to-near infrared range and show a relatively low melting point. Nanostructures made of such poor metals are thus interesting building blocks for spectral-selective thermo-optical devices based on the optical contrast between their solid and liquid phases.

The realization of robust thermo-optical devices requires embedding the nanostructures into stable matrices, with a higher melting point than the metal. The matrix acts as an inert mould trapping the nanostructures, which can be molten and solidified reversibly without relevant changes in their size, shape, and distribution during heating-cooling cycles.[13–20] The physical properties of Bi nanostructures embedded in such robust matrices have been characterized upon heating-cooling cycles using different techniques including Raman, X-ray, and optical transmission.[12,21–24] The embedded nanostructures always show a higher melting temperature compared to the solidification one; therefore, giving rise to characteristic hysteresis loops of the measured physical property as a function of the temperature that have been explained by superheating and supercooling phenomena (see Refs. 22 and 23 and references therein). In particular, a hysteretic response has been observed for the optical transmission of Bi nanoparticles (NPs) embedded in germanate glasses or in amorphous aluminium oxide. However, the results reported so far on the thermo-optical response of embedded Bi NPs have been obtained at a single visible wavelength (560 nm). Due to the rich plasmonic-like optical features of solid Bi NPs that have been recently observed in the visible and near infrared,[25] an exploration of the thermo-optical response of Bi NPs in a broad spectral range is necessary to develop the full potential of spectral-selective Bi-based thermo-optical devices. Therefore in this work, the thermo-optical response of Bi NPs embedded in a germanate glass (known for its high mechanical strength, chemical durability, and thermal stability) is studied in the visible and near infrared.

A Bi-doped germanate glass with molar composition 76 GeO_2–5 Al_2O_3–19 Na_2O, to which 5% in weight (1 mol. %) of Bi_2O_3 was added, was prepared as explained in Ref. 23. Less than 1 mm-thick samples of this glass were cut and polished for optical measurements. While some samples were

[a)]Author to whom correspondence should be addressed. Electronic mail: miguel.jimenez@csic.es
[b)]Present address: Centre de Recherche Paul Pascal, CNRS, Université de Bordeaux, UPR 8641, 115 Avenue Dr Albert Schweitzer, 33600 Pessac, France.

kept without annealing (they will be called hereafter: "as-prepared Bi-doped glass"), a post-annealing treatment was performed for 30 min at 773 K on other samples of this Bi-doped germanate glass in order to induce the formation of Bi NPs embedded in the matrix ("Bi NPs: glass"). For the sake of comparison, an undoped germanate glass was also fabricated using the same procedure as above without adding Bi_2O_3 to the reagent mixture ("pure glass"). Optical transmission spectra at normal incidence (0°) were measured at room temperature in the range 200–1700 nm using a Varian Cary 5000 UV–VIS–NIR spectrophotometer. Additionally, spectroscopic ellipsometry measurements were performed at room temperature at several incident angles (45°, 55°, 65°, and 75°) in the range from 300 to 1700 nm using a J. A. Woollam VASE spectroscopic ellipsometer. The simultaneous analysis of the spectroscopic ellipsometry and transmittance data was performed using the WVASE32 software (Woollam Co. Inc.).

The optical transmission spectra of the as-prepared Bi-doped glass and of the pure glass are shown in Fig. 1(a). The presence of Bi in the glass produces a small shift of the absorption edge towards longer wavelengths. In addition, two weak absorption bands appear in the visible region. The band centred at around 500 nm might be ascribed to bismuth species (ions and/or ion clusters) with low valence state,[26] the other one at around 680 nm is related to the glass network since it also appears in the non-doped glass. The (post-annealed) Bi NPs:glass is dark, as seen in the photographs included in Fig. 1(a), and its transmission is lower than that of the as-prepared Bi-doped glass in the whole wavelength range (Fig. 1(a)). This lower transmittance is related to the presence of Bi NPs, which have been observed by High Resolution Transmission Electron Microscopy (HRTEM) studies and Raman spectroscopy.[23] A HRTEM image is also shown in Fig. 1(a). From the analysis of the HRTEM images, the NPs crystalline structure was observed and it was determined that the they are spherical in shape, the diameter distribution being centred around 5 nm with a full width half maximum of about 6 nm.[23] Raman spectroscopy confirmed the presence of metallic Bi in the annealed samples.[23] It is noteworthy to point out that no Raman band associated to the presence of bismuth oxides was observed.[27]

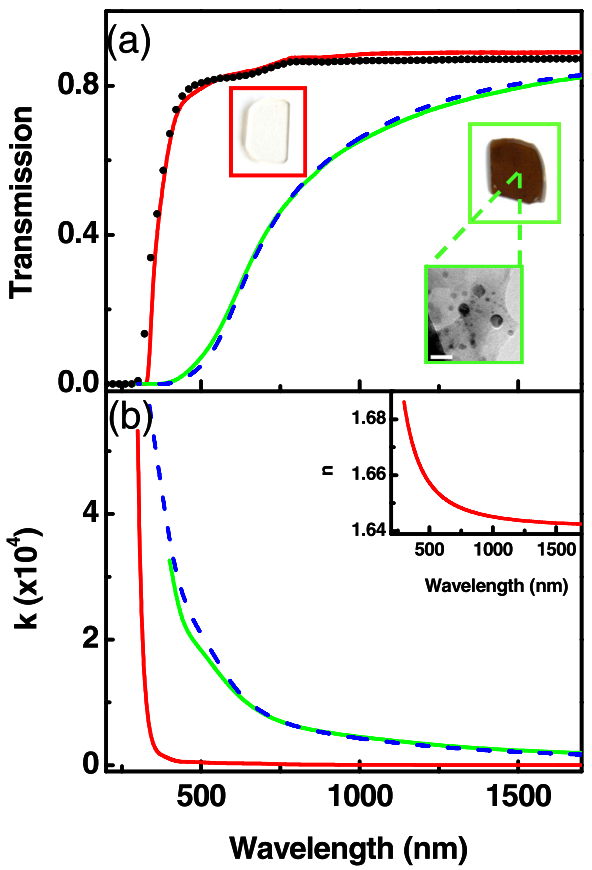

FIG. 1. (a) Optical transmission spectra of the pure germanate glass (black circles), the as-prepared Bi-doped germanate glass (red curve), the Bi NPs: germanate glass (green curve), and Maxwell-Garnett fit of the latter curve (dashed blue curve). The images show pieces of the as-prepared Bi-doped germanate (transparent) and the Bi NPs:germanate (dark) glasses. For the latter, a HRTEM image showing Bi NPs is included (the scale bar is 20 nm long). (b) Extinction coefficient (k) for the as-prepared Bi-doped germanate (red curve) and for the (green curve) Bi NPs:germanate glasses. The k spectrum obtained from Maxwell-Garnett modelling is also included (dashed blue curve). The inset shows the refractive index (n) that is the same for both the as-prepared Bi-doped germanate and Bi NPs:germanate glasses for wavelengths above 400 nm.

The dielectric function (refractive index (n) and extinction coefficient (k)) for both the as-prepared Bi-doped glass and the Bi NPs:glass are shown in Fig. 1(b). The k spectrum of the as-prepared Bi-doped glass up to 300 nm shows a sharp absorption edge, while that of the Bi NPs:glass evidences the strong absorption enhancement as a result of the formation of the Bi NPs. In contrast, both glasses present similar n spectra (inset of Fig. 1(b)). Note that the n and k values for the Bi NPs:glass have been only determined for wavelengths above 400 nm. It has been not possible to determine them for shorter wavelengths due to the zero transmission of the glass.

The Maxwell-Garnett effective medium formalism assuming spherical NPs has been used to model the room-temperature optical transmission of the Bi NPs:glass.[28] This approach should be satisfactory, since the NPs can be assumed to be far enough one from another to prevent mutual interaction and small enough to be considered as quasi static dipoles.[29,30] For the matrix, the dielectric function obtained for the as-prepared Bi-doped glass has been used. For the Bi NPs, the Bi dielectric function of bulk polycrystalline thin films at room temperature, recently reported in Ref. 25, has been used. Therefore, the only parameter to fit is the NP volume fraction (f). The best fit of the experimental transmission at room temperature gives a value for f of 1.26×10^{-4}, that shows that we are in a very dilute NPs regime. It can be estimated that the mass of Bi forming the NPs is 0.03 mg for each 100 mg of glass, that is, about only 0.7% of the Bi content is forming the observed NPs. We have investigated the influence of the particle size and size distribution in the results of Maxwell-Garnett calculations using the customary finite-size corrections, and it has been found that it is negligible for sizes larger than 5 nm. The modelled best-fit optical transmission and effective extinction coefficient (k_{eff}) are plotted in Figs. 1(a) and 1(b). The calculated values are in very good agreement with the measured values showing that the physical behaviour of the Bi NPs:glass is well described by the model.

Then, the optical transmission measurements in the range from 400–800 nm were performed as a function of the temperature between 300 and 700 K using a home-made oven inside a vacuum chamber with a base pressure of 0.1 Pa, with the heating-cooling cycles performed at 10 K min^{-1}. The sample was illuminated at normal incidence by a tungsten-halogen lamp. The light transmitted by the sample was collected by a monochromator and an attached photomultiplier. Fig. 2 shows the evolution with temperature of the optical transmission of the Bi NPs:glass at several wavelengths during a heating-cooling cycle. A hysteresis transmission-temperature loop is observed at each wavelength. This behaviour is not found for the as-prepared Bi-doped glass, therefore it should be related to the Bi NPs formed during the annealing.[23] For all the studied wavelengths, as the temperature increases during the heating cycle the transmission decreases slowly. At about 593 K, a sharp change of the transmission is observed and the transmission either increases (for $\lambda < 600$ nm) or decreases (for $\lambda > 600$ nm). In the cooling part of the cycle, the transmission first increases with decreasing the temperature until another sharp change occurs (decreases for $\lambda < 600$ nm and increases for $\lambda > 600$ nm) at around 366 K, until the initial transmission value is achieved. Note that the temperature at which the transition takes place is always the same independently of the wavelength. These sharp transmission changes have been ascribed to the melting and solidification of the embedded Bi NPs, this conclusion being supported by Raman measurements in this glass.[23] It is worth noting that Raman spectroscopy accounts well for Bi NPs melting and solidification processes, as we demonstrated in Bi NPs-doped Ge thin films in which X-ray diffraction measurements were also performed.[21] It is seen that the NPs melting temperature is higher than that of bulk Bi and the solidification temperature is lower. Such hysteretic behavior is well known to occur in metallic NPs and has been explained from thermodynamic considerations that take into account the size of the NPs and solid NP-matrix and liquid NP-matrix interfacial energy values.[31]

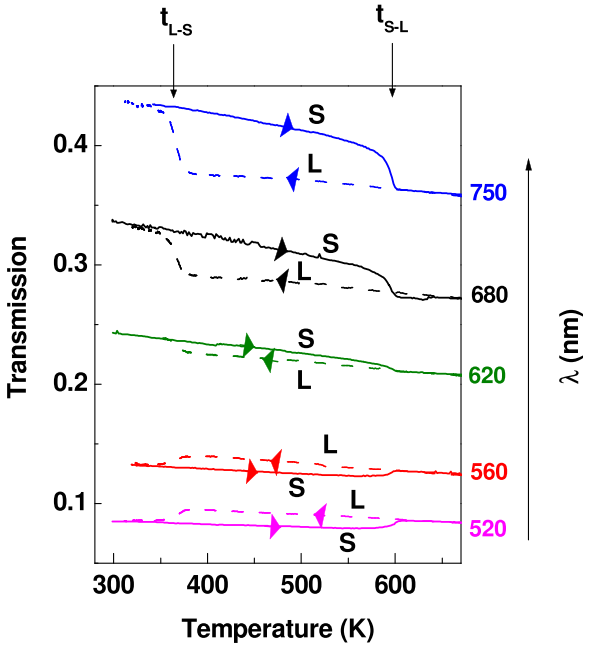

FIG. 2. Transmission evolution as a function of the temperature of the Bi NPs: germanate glass, during heating (continuous line) and cooling (dashed line). The wavelengths at which the transmission is monitored are indicated on the right margin. The solid to liquid transition (t_{S-L}) takes place at 593 K during heating. The liquid to solid (t_{L-S}) transition takes place at 366 K during cooling. **S** indicates that the NPs are in the solid state during most of the heating part of the cycle, and **L** that the NPs are mainly in the liquid state during the cooling part of the cycle.

The transmission spectrum of the glass with liquid Bi NPs just after melting (at 608 K) crosses that of the glass with solid Bi NPs just before melting (at 554 K) at 593 nm. We have plotted in Fig. 3, the *transmission contrast* defined as $(T_{liq} - T_{sol})/T_{sol}$, where T_{liq} is the transmission of the glass with liquid Bi NPs and T_{sol} is the transmission of the glass with solid Bi NPs. The transmission contrast changes from positive to negative at 593 nm, where it cancels, and the maximum absolute contrast values take place at 400 and 800 nm, reaching values close to 12%. These observations agree with the wavelength dependence of the transmission-temperature loops shown in Fig. 2.

To ascertain the origin of the wavelength dependence of the transmission contrast, which has never been reported before, the optical transmission of the Bi NPs:glass, containing either solid or liquid Bi NPs, has been determined at 385 K. At this temperature, both the optical response of the glass with solid Bi NPs and of the glass with liquid Bi NPs (in a supercooled state) can be measured, upon recording the transmission in the heating part and cooling part of the cycle, respectively. Fig. 3 also shows five-point transmission spectra obtained at 385 K, one spectrum corresponding to the glass with solid Bi NPs and the other to the glass with liquid Bi NPs, both being plotted from the data of Fig. 2. A change in transmission contrast from positive to negative upon increasing the wavelength is evidenced. As the dielectric properties of the matrix at a given temperature are likely the same whether the Bi NPs are solid or liquid, the measured transmission contrast at 385 K can be ascribed to a change in the properties of the Bi NPs upon melting-solidification. In order to further identify this change, the transmittance spectra of the Bi NPs:glass at 385 K, containing solid Bi NPs on the one hand, and liquid Bi NPs on the other, has been modelled using the Maxwell-Garnett formalism for spherical nanoparticles. At this temperature, the dielectric properties of both the matrix and solid Bi NPs are very similar to those at room temperature. Therefore, the room temperature dielectric function of the as-prepared Bi-doped glass shown in Fig. 1(b) and the room temperature dielectric function of solid Bi reported in Ref. 25 have been used for the matrix and solid Bi NPs, respectively. The Bi dielectric function reported in Ref. 32 has been used for the liquid Bi NPs. The NP volume fraction f has been adjusted to fit the corresponding experimental sets of transmission values. The resulting curves are also plotted in Fig. 3. Crossing of both curves is observed to occur at 608 nm, thus showing a good agreement with the observed experimental behavior. The obtained f values for solid and liquid Bi NPs are 1.23×10^{-4} and 1.19×10^{-4}, respectively. Both are very similar to the value of 1.26×10^{-4} obtained for the room temperature transmission fit. Therefore, we propose that the wavelength dependence of the transmission contrast of the Bi NPs:glass can be ascribed to the change in the dielectric function of the Bi

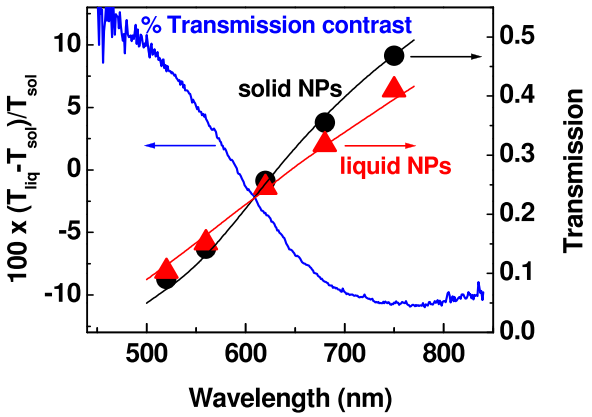

FIG. 3. Percent optical transmission contrast for the Bi NPs: germanate glass between the glass with liquid NPs and the glass with solid NPs as a function of wavelength obtained from the experimental transmission spectra at 554 and 608 K (blue curve). Transmission values taken from the transmission-temperatures cycles of Fig. 2 at 385 K during heating (before NPs melting, black circles) and cooling (after NPs melting and before NPs solidification, red triangles), Maxwell-Garnett fits to both sets of transmission values (full lines).

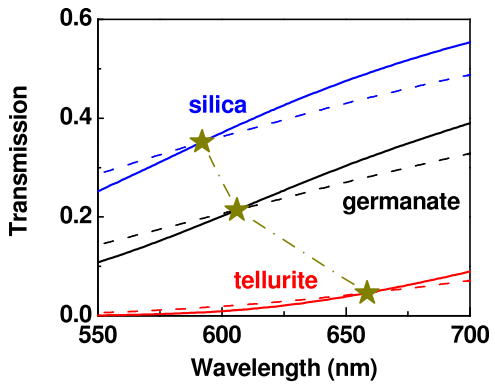

FIG. 4. Simulated (Maxwell-Garnett) transmission spectra of Bi NPs: matrix glasses, with solid (full lines) and liquid (dashed lines) spherical NPs within matrices of different refractive indices (silica, germanate, tellurite). The volume fraction f is that measured in this work. Stars indicate the crossing wavelength (dashed-dotted line is a guide for the eyes).

NPs when their melting takes place (their shape, size and volume fraction being unchanged). These changes alter the optical response of the Bi NPs, which drives the extinction in the Bi NPs:glass. From the dielectric functions of solid[22] and liquid Bi,[32,33] it comes that a spherical solid and liquid Bi NPs embedded in the glass should present a plasmonic-like resonance (as a result of an interband polaritonic behaviour[34]) peaking in the near ultraviolet,[22] and a Drude-like plasmon resonance peaking in the mid ultraviolet, respectively. Due to the high dielectric losses in both solid and liquid Bi, damping effects make the tail of these resonances extend toward the near infrared, thus allowing solid and liquid Bi NPs to absorb light in this range. In this context, the transmission contrast can be linked with the difference in the optical absorption by the solid and liquid Bi NPs, a zero contrast value being attributed to the crossing of the resonance tails of solid and liquid Bi NPs.

In conclusion, the optical transmission of the Bi NPs:germanate glass can be tuned as a function of the temperature. The transmission contrast, which has been measured in the visible-to-near infrared range, is wavelength-dependent and changes from positive to negative upon increasing the wavelength. Furthermore, from the previous interpretation of the obtained results, it comes that the wavelength-dependence of the transmission contrast can be tailored by changing the dielectric function of the matrix, i.e., by modifying the glass composition. In Fig. 4, the transmission of spherical Bi NPs (solid and liquid, calculated in the Maxwell-Garnett formalism) embedded in different host glasses is plotted. The behaviour of the present Bi NPs:germanate glass is compared to that of Bi NPs embedded in a glass matrix with a lower refractive index, such as silica,[35] or with a higher refractive index, such as a tellurite-based glass,[36] both of them with the same volume fraction f as in the Bi NPs:germanate glass. It is evidenced that the spectral features of the transmission contrast between the glass with liquid Bi NPs and the glass with solid Bi NPs strongly depend on the refractive index of the glass matrix. For instance, the wavelength value at which the contrast changes from positive to negative increases as the refractive index of the matrix increases in a wide wavelength range from 590 to 645 nm. Preliminary simulations using the Maxwell-Garnett theory also show that further tailoring of the wavelength–dependence of the transmission contrast can be achieved by controlling the volume fraction occupied by the Bi NPs in the glass matrix and the Bi NPs size and shape.[34] Tailoring of the Bi NP melting and solidification temperatures (and therefore the hysteresis cycle amplitude), as well as the optical contrast at a single wavelength (560 nm) has already been reported, in Bi NPs: amorphous Al_2O_3 thin films grown by pulsed laser deposition.[22,25] The observed wavelength dependence of the transmission contrast, together with the possibility of tailoring its spectral features in a broad spectral range, as predicted by calculations, suggests that Bi NPs-based materials have a strong potential for the development of wavelength-selective thermo-optical modulators and filters in a broad range from the visible to the near infrared. Finally, note that the use of other poor plasmonic metals, such as Ga or Sn, with low melting point will broaden the range of potential devices.

This work has been partially supported by FP7-NMP-2010-Eu-Mexico Grant Agreement No. 263878: Functionalities of Bismuth based Nanostructures (BisNano) and by from the Spanish Ministry of Economy and Competitiveness under Project No. TEC2012-38901-C02-01. J.T. acknowledges a Juan de la Cierva Grant No. JCI-2009–05098. We are also indebted to Dr. C. Ricolleau (Laboratoire Matériaux et Phénomènes Quantiques, Université Paris 7-Denis Diderot, France) for the TEM photograph.

[1]K. F. MacDonald, Z. L. Samson, M. I. Stockman, and N. I. Zheludev, Nat. Photonics **3**, 55 (2009).
[2]G. Garcia, R. Buonsanti, E. L. Runnerstrom, R. J. Mendelsberg, A. Llordes, A. Anders, T. J. Richardson, and D. J. Milliron, Nano Lett. **11**, 4415 (2011).
[3]N. K. Emani, T. F. Chung, X. J. Ni, A. V. Kildishev, Y. P. Chen, and A. Boltasseva, Nano Lett. **12**, 5202 (2012).
[4]Z. L. Samson, K. F. MacDonald, F. De Angelis, B. Gholipour, K. Knight, C. C. Huang, E. Di Fabrizio, D. W. Hewak, and N. I. Zheludev, Appl. Phys. Lett. **96**, 143105 (2010).
[5]C. Langhammer, E. M. Larsson, B. Kasemo, and I. Zoric, Nano Lett. **10**, 3529 (2010).

[6]H. N. S. Krishnamoorthy, S. R. You Zhou, E. Narimanov, and V. M. Menon, Appl. Phys. Lett. **104**, 121101 (2014).
[7]M. G. Blaber, M. D. Arnold, and M. J. Ford, J. Phys.: Condens. Matter **22**, 143201 (2010).
[8]G. V. Naik, V. M. Shalaev, and A. Boltasseva, Adv. Mater. **25**, 3264 (2013).
[9]S. R. C. Vivekchand, C. J. Engel, S. M. Lubin, M. G. Blaber, W. Zhou, J. Y. Suh, G. C. Schatz, and T. W. Odom, Nano Lett. **12**, 4324 (2012).
[10]K. F. MacDonald, V. A. Fedotov, S. Pochon, K. J. Ross, G. C. Stevens, N. I. Zheludev, W. S. Brocklesby, and V. I. Emel'yanov, Appl. Phys. Lett. **80**, 1643 (2002).
[11]M. Schwind, V. P. Zhdanov, I. Zoric, and B. Kasemo, Nano Lett. **10**, 931 (2010).
[12]E. Haro-Poniatowski, R. Serna, A. Suarez-Garcia, and C. N. Afonso, Nanotechnology **16**, 3142 (2005).
[13]A. M. Malvezzi, M. Allione, M. Patrini, A. Stella, P. Cheyssac, and R. Kofman, Phys. Rev. Lett. **89**, 087401 (2002).
[14]K. F. MacDonald, V. A. Fedotov, and N. I. Zheludev, Appl. Phys. Lett. **82**, 1087 (2003).
[15]R. Lopez, L. A. Boatner, T. E. Haynes, R. F. Haglund, and L. C. Feldman, Appl. Phys. Lett. **85**, 1410 (2004).
[16]E. A. Olson, M. Y. Efremov, M. Zhang, Z. Zhang, and L. H. Allen, J. Appl. Phys. **97**, 034304 (2005).
[17]G. Kellermann and A. F. Craievich, Phys. Rev. B **65**, 134204 (2002).
[18]G. Kellermann and A. F. Craievich, Phys. Rev. B **78**, 054106 (2008).
[19]H. Amekura, M. Tanaka, Y. Katsuya, H. Yoshikawa, H. Shinotsuka, S. Tanuma, M. Ohnuma, Y. Matsushita, K. Kobayashi, C. Buchal *et al.*, Appl. Phys. Lett. **96**, 023110 (2010).
[20]H. Amekura, M. L. Sele, N. Ishikawa, and N. Okubo, Nanotechnology **23**, 095704 (2012).
[21]E. Haro-Poniatowski, R. Serna, C. N. Afonso, M. Jouanne, J. F. Morhange, P. Bosch, and V. H. Lara, Thin Solid Films **453–454**, 467 (2004).
[22]E. Haro-Poniatowski, R. Serna, M. Jiménez de Castro, A. Suarez-Garcia, C. N. Afonso, and I. Vickridge, Nanotechnology **19**, 485708 (2008).
[23]E. Haro-Poniatowski, M. Jiménez de Castro, J. M. Fernández Navarro, J. F. Morhange, and C. Ricolleau, Nanotechnology **18**, 315703 (2007).
[24]H. H. Andersen and E. Johnson, Nucl. Instrum. Methods B **106**, 480 (1995).
[25]J. Toudert, R. Serna, and M. Jiménez de Castro, J. Phys. Chem. C **116**, 20530 (2012).
[26]B. B. Xu, S. F. Zhou, D. Z. Tan, Z. L. Hong, J. H. Hao, and J. R. Qiu, J. Appl. Phys. **113**, 083503 (2013).
[27]L. Kumari, J.-H. Lin, and Y.-R. Ma, J. Phys. D: Appl. Phys. **41**, 025405 (2008).
[28]M. Y. Koledintseva, S. K. R. Chandra, R. E. DuBroff, and R. W. Schwartz, Prog. Electromag. Res. **66**, 213 (2006).
[29]S. Camelio, D. Babonneau, T. Girardeau, J. Toudert, F. Lignou, M.-F. Denanot, N. Maître, A. Barranco, and P. Guérin, Appl. Opt. **42**, 674 (2003).
[30]V. Myroshnychenko, J. Rodriguez-Fernandez, I. Pastoriza-Santos, A. M. Funston, C. Novo, P. Mulvaney, L. M. Liz-Marzan, and F. J. G. de Abajo, Chem. Soc. Rev. **37**, 1792 (2008).
[31]Q. Xu, I. D. Sharp, C. W. Yuan, D. O. Yi, C. Y. Liao, A. M. Glaeser, A. M. Minor, J. W. Beeman, M. C. Ridgway, P. Kluth *et al.*, Phys. Rev. Lett. **97**, 155701 (2006).
[32]S. Dogel, D. Nattland, and W. Freyland, Phys. Rev. B **72**, 085403 (2005).
[33]T. Inagaki, E. T. Arakawa, A. R. Cathers, and K. A. Glastad, Phys. Rev. B **25**, 6130 (1982).
[34]J. Toudert, Nanotechnol. Rev. **3**, 223 (2014).
[35]P. Chindaudom and K. Vedam, Appl. Opt. **32**, 6391 (1993).
[36]D. Munoz-Martin, J. M. Fernandez-Navarro, J. Gonzalo, G. Jose, A. Jha, J. L. G. Fierro, C. Domingo, and J. Garcia-Lopez, Thin Solid Films **520**, 131 (2011).